Modified Non-isolated Bidirectional DC–DC Converter for Regenerative Braking for Electric Vehicle Applications

Mukesh Kumar, Kunal Kumar, and Kalpana Chaudhary

Abstract Electric vehicles (EVs) have a driving range constrained by space and weight. Regenerative braking using a bidirectional converter in EVs can increase the driving range by efficiently using the energy stored in the battery bank. A modified non-isolated bidirectional DC–DC converter is proposed in this paper. The modified converter operates basically in two modes, viz. motoring (boost) mode and regenerative braking (buck) mode. The voltage gain of the proposed converter is found to be twice of the conventional bidirectional DC–DC converter in motoring mode, whereas it is half of the conventional bidirectional DC–DC converter in braking mode. It is also envisaged that as the gain performance of the modified converter is much better than the conventional converter, it can work in a wide voltage range. Closed-loop operation of the modified converter is demonstrated feeding a permanent magnet DC (PMDC) motor, and its energy recovery due to regenerative braking is demonstrated. A laboratory prototype is developed to validate the operation of the proposed converter.

Keywords Battery · Bidirectional DC–DC converter · Electric vehicle · PMDC motor

1 Introduction

The rising energy demand in the automotive sector can no longer be sustained by conventional energy resources due to increasing cost, pollution, and availability. The greenhouse gases emitted from conventional sources are degrading the environmental condition across the globe. Thus, renewable energy sources comprising wind energy, solar energy, fuel cell, photovoltaic, and so on have gained popularity [1, 2]. The intermittent availability of renewable resources can be resolved by using energy storage devices as it increases its stability and reliability [3]. The bidirec-

M. Kumar (✉) · K. Kumar · K. Chaudhary
Indian Institute of Technology (BHU), Varanasi, Varanasi, India
e-mail: mukeshk.rs.eee16@itbhu.ac.in

S. Mohapatro and J. Kimball (eds.), *Proceedings of Symposium on Power Electronic and Renewable Energy Systems Control*, Lecture Notes in Electrical Engineering 616,
https://doi.org/10.1007/978-981-16-1978-6_7

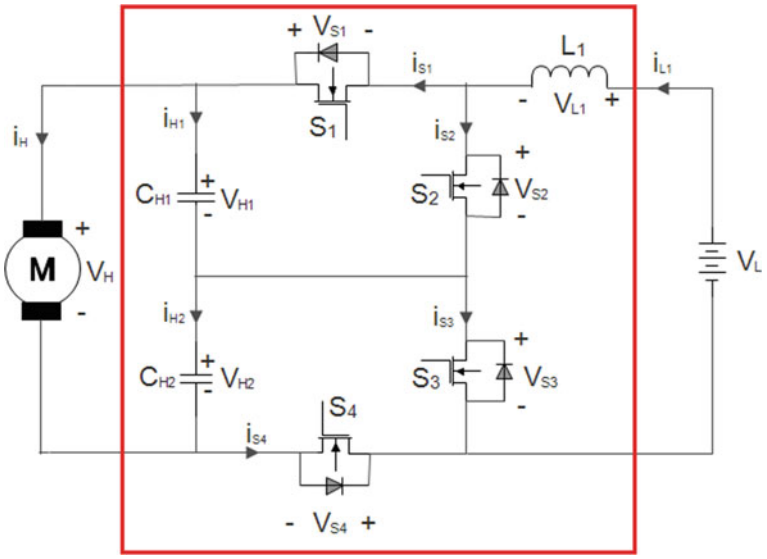

Fig. 1 Modified bidirectional DC–DC converter

tional DC–DC converter can transfer the power in both directions; these converters are widely used for renewable energy hybrid power systems, uninterrupted power supplies (UPS) [4–6], and hybrid electric vehicle system [7, 8], battery chargers [9, 10], fuel cell hybrid systems [11, 12], and other applications. The development of bidirectional DC–DC converters has recently become increasingly important for clean energy vehicle applications with cold starting and battery recharging [13, 14]. In the conventional buck–boost converter, the voltage gain is limited by switching losses and the equivalent series resistance (ESR) of capacitors and inductors. Therefore, conventional buck–boost converter is not preferred in applications with wide range of voltage gain.

The proposed modified bidirectional DC–DC converter is shown in Fig. 1. The voltage gain of modified converter is two times that of conventional converter during step-up mode and is half during step-down mode. For analysis, following conditions are assumed: (i) R_{DS} of the MOSFETs and the ESR in capacitors are not considered. (ii) The voltages across capacitors C_{H1}, C_{H2}, and C_L are treated as constant. (iii) $C_{H1} = C_{H2}$.

This paper is organized as follows: Sect. 2 describes the working and operating principle of converter in step-up mode, Sect. 3 deals with the step-down operation and working, Sect. 4 contains the simulation results and discussion, Sect. 5 contains the hardware results and discussion. Lastly, Sect. 6 draws a conclusion of this work.

2 Step-Up Mode of Modified Converter

As the circuit has four switches, namely S_1, S_2, S_3, and S_4. For control of the switches S_2 and S_3, PWM techniques are used. The switches S_1 and S_2 are off all the time. The operating principle is described using Fig. 2.

2.1 Mode 1, [t_0 , t_1]

The equivalent circuit of converter for step-up mode is shown in Fig. 1 switches S_1 and S_4 which are turned OFF while switches S_2 and S_3 are turned ON. Thus, the input inductor (L) voltage is given as:

$$V_L^{\mathrm{I}} = V_L \tag{1}$$

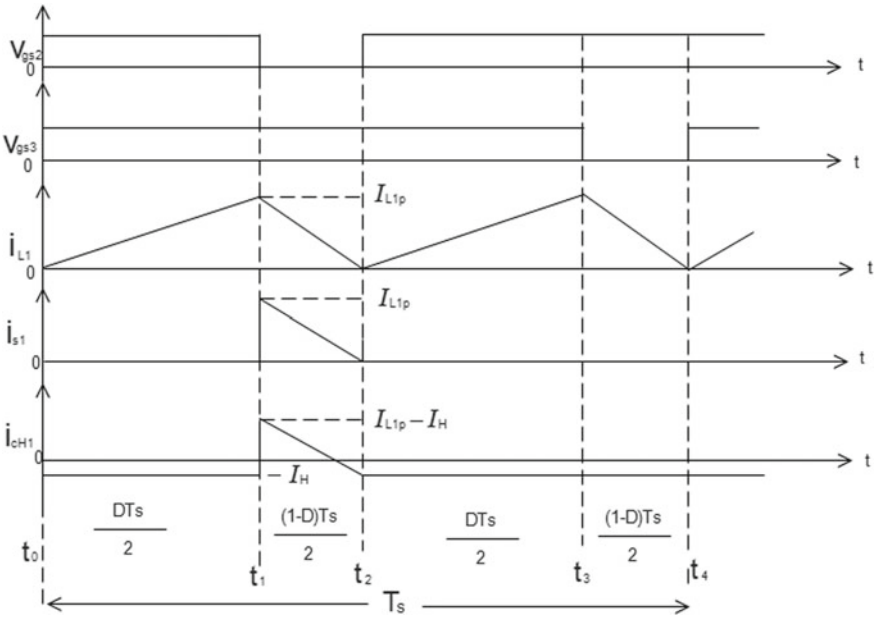

Fig. 2 Operation of the proposed converter

The inductor current is given by:

$$i_L^{\mathrm{I}}(t) = i_L(t_o) + \frac{V_L}{L}(t - t_o) \tag{2}$$

2.2 Mode 2, [t_1, t_2]

The switch S_3 is turned ON and the switches, S_1, S_2, and S_4 are turned OFF. The antiparallel diode of S_1 is always forward biased. Thus, the input inductor (L) voltage is given as:

$$V_L^{\mathrm{II}} = V_L - \frac{V_H}{2} \tag{3}$$

The inductor current is given by:

$$i_L^{\mathrm{II}}(t) = i_L(t_1) + \frac{1}{L}\left(V_L - \frac{V_H}{2}\right)(t - t_1) \tag{4}$$

2.3 Mode 3, [t_2, t_3]

The operation in this mode is similar to mode 1. Thus, the input inductor (L) voltage is given as:

$$V_L^{\mathrm{III}} = V_L \tag{5}$$

The inductor current is given by:

$$i_L^{\mathrm{III}} = i_L(t_2) + \frac{V_L}{L}(t - t_2) \tag{6}$$

2.4 Mode 4, [t_3, t_4]

The switch S_2 is turned ON, and the switches S_1, S_3 and S_4 are turned OFF. Here, the antiparallel diode of S_4 is always forward biased. Thus, the input inductor (L) voltage is found as:

$$V_L^{\mathrm{IV}} = V_L - \frac{V_H}{2} \tag{7}$$

The inductor current is given by:

$$i_L^{\mathrm{IV}}(t) = i_L(t_3) + \frac{1}{L}\left(V_L - \frac{V_H}{2}\right)(t - t_3) \tag{8}$$

Applying Volt–Second balance principle on the inductor L, the following equation is obtained:

$$\begin{aligned} V_L = {} & \frac{DT_s}{2}V_L + \frac{(1-D)T_s}{2}\left(V_L - \frac{V_H}{2}\right) \\ & + \frac{DT_s}{2}V_L + \frac{(1-D)T_s}{2}\left(V_L - \frac{V_H}{2}\right) = 0 \end{aligned} \tag{9}$$

Thus, on solving (9), the voltage gain (G) is obtained as

$$G_{\text{step-up}} = \frac{V_H}{V_L} = \frac{2}{(1-D)} \tag{10}$$

The peak value of current in inductor i_L is:

$$I_L = \frac{DT_sV_L}{2L} \tag{11}$$

Applying Ampere–Second balance on the capacitor C_{H1},

$$I_{CH1} = \frac{(1/2)((1-D)T_s/2)I_{LP} - I_HT_s}{T_s} \tag{12}$$

So, the normalized inductor time constant is:

$$I_{L,P} = \frac{4I_H}{(1-D)} = \frac{4V_H}{(1-D)R_H} \tag{13}$$

$$\tau_{LH} = \frac{L}{R_HT_s} = \frac{Lf_s}{R_H} \tag{14}$$

On substituting (10), (11), and (12) into (13), the boundary of τ_{LH} can be obtained as follows:

$$\tau_{LH,B} = \frac{D(1-D)^2}{16} \tag{15}$$

If $\tau_{LH,B}$ is smaller than τ_{LH}, the modified converter will operate in CCM in the step-up mode.

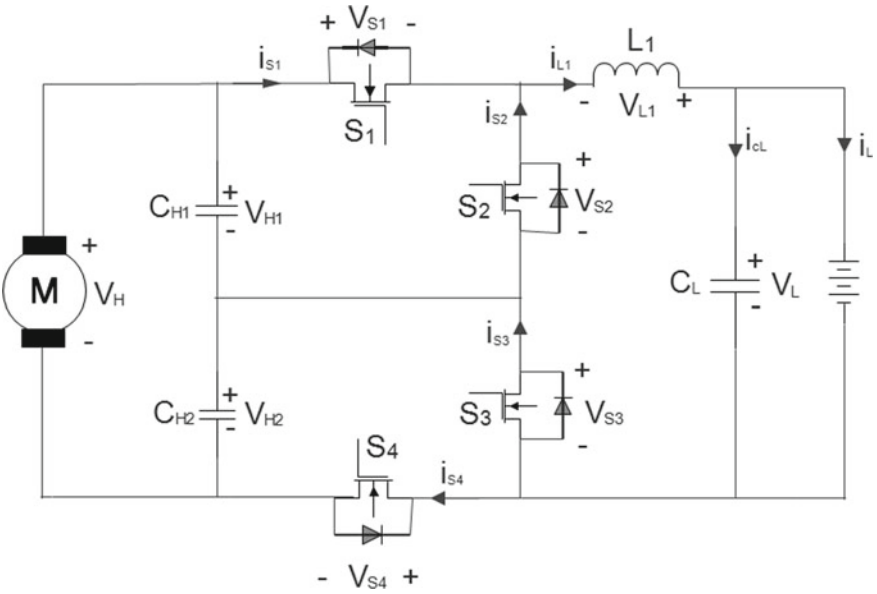

Fig. 3 Equivalent circuit of the modified converter in the step-down mode

3 Step-Down Mode of Modified Converter

Figure 3 shows equivalent circuit of the modified converter in step-down mode. Switches S_1 and S_4 are switched according to the PWM technique, and switches S_2 and S_3 are OFF in this mode.

3.1 Mode 1, [t_0 , t_1]

In this mode, switch S_1 is turned on and switches S_2, S_3 and S_4 are turned off. Also, the diode with switch S_3 is forward biased. Thus, the input inductor (L) voltage is given as:

$$V_L^{\mathrm{I}} = \frac{V_H}{2} - V_L \tag{16}$$

The inductor current is given by:

$$i_L^{\mathrm{I}}(t) = i_L(t_0) + \frac{1}{L}\left(\frac{V_H}{2} - V_L\right)(t - t_0) \tag{17}$$

3.2 Mode 2, [t_1 , t_2]

All the switches S_1, S_2, S_3, and S_4 are turned off. The diode with switch S_2 and S_3 is forward biased. Thus, the input inductor (L) voltage is given as:

$$V_L^{\mathrm{II}} = -V_L \tag{18}$$

The inductor current is given by:

$$i_L^{\mathrm{II}} = i_L(t_1) - \frac{V_L}{L}(t - t_1) \tag{19}$$

3.3 Mode 3, [t_2 , t_3]

In this mode, switches S_1, S_2 and S_3 are turned OFF while switch S_4 is turned ON. Also, the diode with switch S_2 is forward biased. Thus, the input inductor (L) voltage is given as:

$$V_L^{\mathrm{III}} = \frac{V_H}{2} - V_L \tag{20}$$

The inductor current is given by:

$$i_L^{\mathrm{III}}(t) = i_L(t_2) + \frac{1}{L}\left(\frac{V_H}{2} - V_L\right)(t - t_2) \tag{21}$$

3.4 Mode 4, [t_3 , t_4]

As the operation is similiar as mode 2, thus the input inductor (L) voltage is found as:

$$V_L^{\mathrm{IV}} = -V_L \tag{22}$$

The inductor current is given by:

$$i_L^{\mathrm{IV}} = i_L(t_3) - \frac{V_L}{L}(t - t_3) \tag{23}$$

Applying Volt–Second balance principle on the inductor L, the following equation is obtained:

$$V_L = \frac{DT_s}{2}\left(\frac{V_H}{2} - V_L\right) - \frac{(1-D)T_s}{2}V_L + \frac{DT_s}{2}\left(\frac{V_H}{2} - V_L\right) - \frac{(1-D)T_s}{2}V_L = 0 \tag{24}$$

On solving (24), the voltage gain is obtained as

$$G_{\text{step-down}} = \frac{V_L}{V_H} = \frac{D}{(2)} \tag{25}$$

The peak current of inductor for BCM i_L is given by

$$I_{L,P} = \frac{DT_s}{2L}\left(\frac{V_H}{2} - V_L\right) \tag{26}$$

Applying Ampere–Second balance on the capacitor C_L,

$$I_{CL} = \frac{(1/2)[(DT_s/2) + ((1-D)T_S/2)]I_{LP} - I_L T_s}{T_s} = 0 \tag{27}$$

So, following equation is determined

$$I_{L,P} = 2I_L = \frac{2V_L}{R_L} \tag{28}$$

where R_L is equivalent load resistance. Therefore, the normalized inductor time constant is defined as

$$\tau_{LL} = \frac{L}{R_L T_s} = \frac{Lf_s}{R_L} \tag{29}$$

By using (25), (26), (28) and (29), the value of τ_{LL} is found to be:

$$\tau_{LL,B} = \frac{(1-D)}{4} \tag{30}$$

If $\tau_{LL,B}$ is smaller than τ_{LL}, the modified converter will operate in current continuous mode (CCM) in the step-down mode.

4 Simulation Results

The designed system is simulated in MATLAB–Simulink. Battery voltage is taken as 24 V with initial state of charge (SOC) of 88%. Figure 4 shows battery characteristics and motor speed in motoring and braking mode. It can be seen that during motoring mode speed of motor increases, battery voltage decreases, SOC decreases, and in

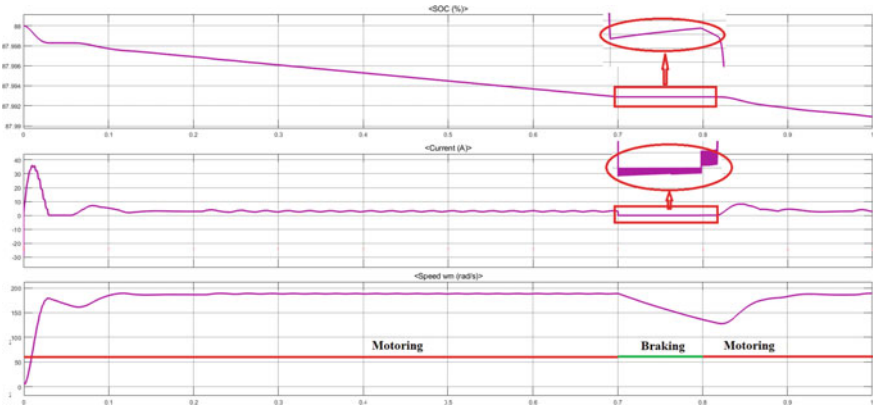

Fig. 4 Simulation result of motoring and braking operation

Table 1 Circuit parameters and its value

Parameters	Notation	Values
Battery voltage	V_L	24 V
Motor voltage	V_H	100 V
Motor power	P_H	0.5 hp
Switching frequency	f_s	40 kHz
High side capacitors	$C_{H1} = C_{H2}$	100 µF
Low side capacitors	C_L	100 µF
Inductor	L	605 µH

regenerative braking mode, current is negative, battery voltage increases and SOC increases. Motoring action is from 0 to 0.7 s and 0.8 to 1 s. Regenerative braking action is from 0.7 to 0.8 s. The converter system model and the implemented PI controller are designed as in [15]. The specification of circuit components is given in Table 1.

The voltage gain in the step-up mode, $G = 4.167$. Substituting it in (10), duty ratio is calculated as 0.52. Substituting $D = 0.52$ in (15), boundary normalized time constant $\tau_{LH,B}$ is obtained as 0.007488. For the converter to operate in CCM mode, we take 10% of full load, therefore $R_H = 268.1\,\Omega$.

When $\tau_{LH} > \tau_{LH,B}$, the modified converter is found to operate in CCM. From (14), the value of input inductor L is calculated as:

$$L * \frac{40,000}{268.1} \geq 0.007488 \tag{31}$$

$L \geq 510\,\mu\text{H}$ (considering 10% of full load to operate in CCM mode). The voltage gain in the step-down mode, $G = 0.24$. Substituting it in (25) yields the duty ratio

as 0.48. Substituting value of D in (30), the boundary normalized time constant $\tau_{LL,B}$ is obtained as 0.13. For the converter to operate in CCM mode, we take 10% of full load, therefore $R_L = 15.44\,\Omega$. When $\tau_{LL} \geq \tau_{LL,B}$, the modified converter operates in CCM. Using (29), the input inductor L is:

$$L * \frac{40,000}{15.44} \geq 0.13 \tag{32}$$

$L \geq 520\,\mu\text{H}$ (considering 10% of full load to operate in CCM mode). Therefore, the input inductor L is selected as 605 μH, for operation in CCM mode and it is selected with extra safety.

5 Experimental Results

Figure 5 shows the experimental results with multiple braking transitions. Channel 1 shows the motor side voltage, Channel 2 shows battery side voltage, Channel 3 shows PWM switching, and Channel 4 shows inductor current. Inductor current falling negative during braking action proofs the regenerative braking action, as energy is being fed to battery and thus charging it. During braking, inductor current increases at first and so the motor voltage, and at last, it tries to follow the reference voltage as can be seen from rise of Channel 1 voltage from Fig. 5. The various parameters of the circuit are mentioned in Table 1. The experimental setup used for testing the prototype is shown in Fig. 6.

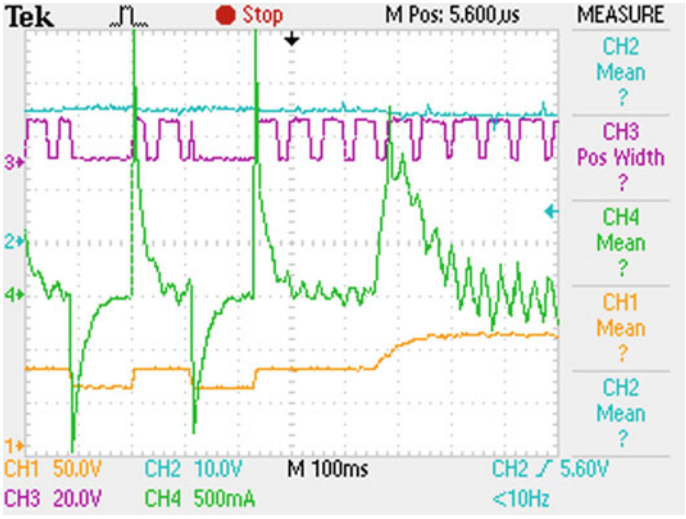

Fig. 5 Experimental result with multiple braking transition

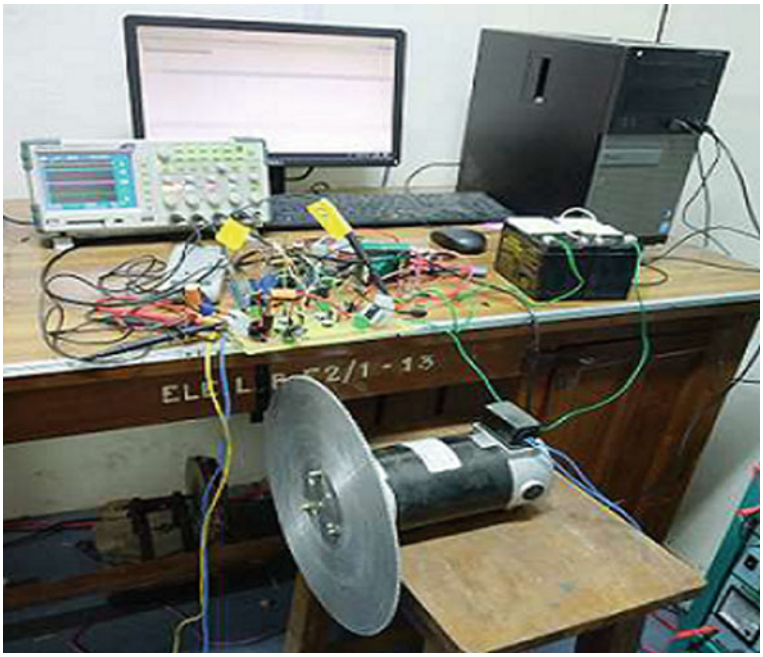

Fig. 6 Complete experiment setup

6 Conclusion

A modified non-isolated bidirectional DC–DC converter is designed and developed in this work. The developed prototype of the converter has been tested for regenerative braking in a wide voltage conversion range. The controller has been found to be working as evident from the results. The switching scheme of converter is found to be easy to implement. From the simulation and experimental results, the bidirectional nature of the converter with motoring and regenerative braking action is found to be working satisfactorily. SOC curve clearly shows the region of discharging and charging of battery during motoring and braking action, respectively.

References

1. Z. Zhang, O.C. Thomsen, M.A.E. Andersen, H.R. Nielsen, Dual-input isolated full-bridge boost DC-DC converter based on the distributed transformers. IET Power Electron. **5**(7), 1074–1083 (2012)
2. Y.P. Hsieh, J.F. Chen, T.J. Liang, L.S. Yang, Analysis and implementation of a novel single-switch high step-up DC-DC converter. IET Power Electron. **5**(1), 11–21 (2012)
3. C.C. Lin, L.S. Yang, G.W. Wu, Study of a non-isolated bidirectional DC-DC converter. IET Power Electron. **6**(1), 30–37 (2013)

4. A. Nasiri, Z. Nie, S.B. Bekiarov, A. Emadi, An on-line UPS system with power factor correction and electric isolation using BIFRED converter. IEEE Trans. Ind. Electron. **55**(2), 722–730 (2008)
5. M. Salimi, J. Soltani, G.A. Markadeh, N.R. Abjadi, Indirect output voltage regulation of DC–DC buck/boost converter operating in continuous and discontinuous conduction modes using adaptive back stepping approach. IET Power Electron. **6**(4), 732–741 (2013)
6. L. Schuch, C. Rech, H.L. Hey, H.A. Grundling, H. Pinheiro, J.R. Pinheiro, Analysis and design of a new high-efficiency bidirectional integrated ZVT PWM converter for DC-bus and battery-bank interface. IEEE Trans. Ind. Appl. **42**(5), 1321–1332 (2006)
7. F.Z. Peng, F. Zhang, Z. Qian, A magnetic-less DC-DC converter for dual-voltage automotive systems. IEEE Trans. Ind. Appl. **39**(2), 511–518 (2003)
8. T. Bhattacharya, V.S. Giri, K. Mathew, L. Umanand, Multiphase bidirectional flyback converter topology for hybrid electric vehicles. IEEE Trans. Ind. Electron. **56**(1), 78–84 (2009)
9. S.Y. Lee, G. Pfaelzer, J.D. Wyk, Comparison of different designs of a 42-V/14-V DC/DC converter regarding losses and thermal aspects. IEEE Trans. Ind. Appl. **43**(2), 520–530 (2007)
10. K. Jin, M. Yang, X. Ruan, M. Xu, Three-level bidirectional converter for fuel-cell/battery hybrid power system. IEEE Trans. Ind. Electron. **57**(6), 1976–1986 (2010)
11. G. Ma, W. Qu, G. Yu, Y. Liu, N. Liang, W. Li, A zero-voltage-switching bidirectional DC-DC converter with state analysis and soft switching-oriented design consideration. IEEE Trans. Ind. Electron. **56**(6), 2174–2184 (2009)
12. W.C. Liao, T.J. Liang, H.H. Liang, H.K. Liao, L.S. Yang, K.C. Juang, J.F. Chenl, Study and implementation of a novel bidirectional DC-DC converter with high conversion ratio. IEEE Conf. Power Electron. 134–140 (2011)
13. W. Yu, H. Qian, J.S. Lai, Design of high-efficiency bidirectional DC-DC converter and high-precision efficiency measurement. IEEE Conf. Power Electron. 685–690 (2008)
14. H. Li, F.Z. Peng, J.S. Lawler, A natural ZVS medium-power bidirectional DC-DC converter with minimum number of devices. IEEE Trans. Ind. Electron. **39**(2), 525–535 (2003)
15. H. Sira-Ramirez, Nonlinear P-I controller design for switchmode DC-to-DC power converters. IEEE Conf. Power Electron. 2797–2802 (2011)